Abstract for the 31st International Workshop on Water Waves and Floating Bodies, Plymouth, Michigan, USA, April 3-6, 2016.

On Hydrodynamic Behavior of a Cylindrical Moonpool with an Entrapped Two-Layer Fluid

Xinshu Zhang[1,2*] and Ronald W. Yeung[2†]

[1] School of Naval Architecture, Ocean & Civil Engineering, Shanghai Jiao Tong University, Shanghai, China

[2] Department of Mechanical Engineering, University of California, Berkeley, USA

Highlights:

- *Matched eigenfunction-expansion method with a two-layer fluid model is employed to investigate the hydrodynamic behavior of a floating cylindrical moonpool with an entrapped two-layer fluid.*
- *Parametric studies have been performed to identify the dependence of the heave resonance characteristics on moonpool configuration and density stratification.*

1 Introduction

This paper aims to study the hydrodynamic behavior of a floating cylindrical moonpool (possibly a solar pond) generated by its harmonic, forced heave motion. The "pond" is a large semi-submerged open thin-walled circular cylinder designed for fresh-water storage, in which a certain density stratification is normally expected. Both the fluid motion inside the moonpool or pond and the dynamic behavior of the floating structure can be critical issues. This type of problem was initially studied by Miloh [4] based on an eigenfunction matching method similar to that developed by Yeung [6] and wave exciting forces were computed for 3 modes of motion. However, the density stratification inside the pond and the wall thickness was not modeled in that study.

The hydrodynamic problem of a floating solar pond is very similar to that of a rectangular moonpool. Molin [5] demonstrated a resonance inside the moonpool based on linearized water-wave theory. Yeung & Seah [8] and Faltinsen et al. [2] studied the two-dimensional piston-like wave sloshing inside a moonpool based on a domain decomposition scheme. Mavrakos [3] and Chau & Yeung [1] studied the three-dimensional moonpool/co-axial cylinders geometry. Those studies have been only focused on a single-layer fluid, but density can change because of variations in salinity or temperature in the vertical direction is possible. If a thin pycnocline should exist, we can model it simply as a two-layer fluid with distinct but constant densities in each layer. Two-dimensional moonpool resonance in a stratified flow has been studied by Zhang & Bandyk [9, 10] for different moonpool configurations. A comprehensive treatment of the three-dimensional wave-body interaction in a two-layer fluid can be found in [7].

The focus of the present study is the three-dimensional wave radiation because of heave excitation from the bottom of the finite-thickness vertical cylinder with an opening where fluid density stratification occurs. We first provide the mathematical formulation, followed by a numerical scheme to solve the discretized linear system. A few preliminary results are presented, in particular, the hydrodynamic behavior of the floating solar pond near resonance is examined. Parametric studies are performed to examine the effects of pond geometry and density stratification on the resonant fluid motion and hydrodynamic coefficients. The proposed model is effective in rapidly predicting resonant characteristics for a given moonpool configuration, which can be critical to associated design and optimizations.

*Presenting author. Email: xinshuz@sjtu.edu.cn

†corresponding author (rwyeung@berkeley.edu)

2 Theory and Approach

The hydrodynamic problem induced by a forced small-amplitude heave motion of a finite-thickness walled vertical cylinder ('solar pond') of a finite draft is studied. The fluid stratification inside the solar pond is modeled as a two-layer fluid. The schematic for the problem and coordinate system are illustrated in Fig. 1. Let the Oxy plane be the calm-water surface, (r, θ) be the polar coordinates in the horizontal plane, and the z-axis point upwards from the sea floor. The internal and external radius of the cylinder are a and b, respectively. The wall thickness of circular cylinder is $b - a$. The draft of the floating cylinder is d. The depth of upper and lower layers inside the pond are h_1 and h_2, respectively, with corresponding densities being ρ_1 and ρ_2. with a total internal water depth is $h = h_1 + h_2$. The fluid is assumed to be ideal and the flow irrotational. Heave motion is studied here, the hydrodynamic problem is axisymmetric about $z-$axis and the solution is expected to depend only on z and r.

Let the heave motion of the floating circular cylinder be $\zeta \cos(\omega t)$, where ω is the angular frequency and ζ is the motion amplitude. We assume $\zeta \ll O(d)$. The velocity potential can be written as

$$\Phi(r, \theta, z, t) = \Re\left[-\mathrm{i}\omega\zeta\phi(r, \theta, z)e^{-\mathrm{i}\omega t}\right] \tag{1}$$

where $\phi(r, \theta, z)$ is the spatial velocity potential.

The governing equation for $\phi(r, \theta, z, t)$ is the Laplace equation

$$\left(\frac{\partial^2}{\partial r^2} + \frac{1}{r}\frac{\partial}{\partial r} + \frac{1}{r^2}\frac{\partial^2}{\partial \theta^2} + \frac{\partial^2}{\partial z^2}\right)\phi(r, \theta, z) = 0 \tag{2}$$

Considering the axi-symmetric behavior of the fluid motion, the governing equation can be further simplified to

$$\left(\frac{\partial^2}{\partial r^2} + \frac{1}{r}\frac{\partial}{\partial r} + \frac{\partial^2}{\partial z^2}\right)\phi(r, \theta, z) = 0 \tag{3}$$

The linearized free-surface boundary condition is given by

$$\phi_z - K\phi = 0 \text{ at } z = h_1 + h_2 \tag{4}$$

where $K = \omega^2/g$, and g is the gravitational acceleration.

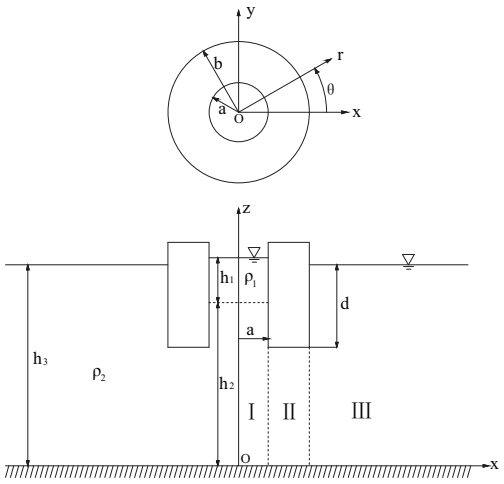

Figure 1: Definition of the problem and coordinate systems

The region of the fluid domain $r \geq 0$ can be divided into three subdomains which include Region I, II, and III (Fig. 1). The spatial velocity potentials in those regions are denoted by $\phi^{I(m)}$, ϕ^{II} and ϕ^{III}, respectively. In region I, $m = 1$ and $m = 2$ represent the solutions for the upper and lower layers, respectively. ϕ^{II} is the velocity potential of the subdomain underneath the cylinder bottom. ϕ^{III} is the velocity potential of the subdomain outside the body. We remark that fluid is treated using a two-layer model in region I, while the other two regions are modeled as a single-layer fluid.

In region I, the interfacial surface boundary conditions can be written as [7]

$$\phi_z^{I(1)} = \phi_z^{I(2)} \text{ at } z = h_2 \tag{5}$$

$$\gamma\left(\phi_z^{I(1)} - K\phi^{I(1)}\right) = \phi_z^{I(2)} - K\phi^{I(2)} \text{ at } z = h_2 \tag{6}$$

where $\gamma = \rho_1/\rho_2$ is the density ratio.

The hydrodynamic problem is axisymmetric about vertical axis $r = 0$, implying

$$\phi_r^{I(m)} = 0 \text{ on } r = 0 \tag{7}$$

The boundary condition at the seabed is given by

$$\phi_z^{I(2)} = 0 \text{ at } z = 0 \tag{8}$$

In addition, $\phi^{I(m)}$ and ϕ^{III} must satisfy the no-flux condition on the solid body boundaries. Leveraging the symmetry property, we can write the vertical-face boundary conditions as

$$\phi_r^{I(m)} = 0 \text{ at } r = a,\ h - d \leq z \leq h \tag{9}$$

$$\phi_r^{III} = 0 \text{ at } r = b,\ h - d \leq z \leq h_3 \tag{10}$$

The velocity potential in region I can be written as

$$\begin{aligned}\phi^{I(m)}(r,z) &= \sum_{j=0}^{\infty} A_j^1 \Lambda^I\left(k_j^{(1)}, r\right) Z^{(m)}\left(k_j^{(1)}, z\right) + \\ &\sum_{j=0}^{\infty} A_j^2 \Lambda^I\left(k_j^{(2)}, r\right) Z^{(m)}\left(k_j^{(2)}, z\right)\end{aligned} \tag{11}$$

where Λ^I and $Z^{(m)}$ are the eigenfunctions in the horizontal and vertical directions, respectively. $Z^{(m)}$ forms an orthogonal set in $[0, h]$. A_j^1 and A_j^2 are unknown coefficients which will be determined by matching fluid velocity and potential at the juncture boundary between regions I and II. $n = 1$ represents the surface wave mode and $n = 2$ denotes the internal wave mode. $k_j^{(n)}, j = 0, 1, ..., \infty$ are the eigenvalues which can be computed by solving the dispersion relations for a two-layer fluid system [10].

The velocity potential for region II should satisfy the Laplace equation

$$\left(\frac{\partial^2}{\partial r^2} + \frac{1}{r}\frac{\partial}{\partial r} + \frac{\partial^2}{\partial z^2}\right)\phi^{II} = 0 \tag{12}$$

with the following boundary conditions

$$\phi_z^{II} = 1 \quad \text{for } a \leq r \leq b,\ z = h - d \tag{13}$$

$$\phi_z^{II} = 0 \quad \text{for } a \leq r \leq b,\ z = 0 \tag{14}$$

The solution in region II can be written as

$$\phi^{II} = \phi^{IIh} + \phi^{IIp} \tag{15}$$

where the homogeneous solution can be expressed as

$$\phi^{IIh}(r,z) = \sum_{i=0}^{\infty} H(\lambda_i, r) Y(\lambda_i, z) \tag{16}$$

with λ_i being the eigenvalues which are computed using

$$\lambda_i = \frac{i\pi}{h-d} \quad \text{for } i = 0, 1, \ldots, \infty \tag{17}$$

The eigenfunction in the horizontal direction is defined by

$$H(\lambda_i, r) = \begin{cases} C_0 \frac{\ln(r/a)}{\ln(b/a)} + D_0 \frac{\ln(b/r)}{\ln(b/a)} & \text{for } i = 0 \\ C_i R_i(r) + D_i R_i^*(r) & \text{for } i \geq 1 \end{cases} \tag{18}$$

with

$$R_i(r) = \frac{K_0(\lambda_i a) I_0(\lambda_i r) - I_0(\lambda_i a) K_0(\lambda_i r)}{K_0(\lambda_i a)\, I_0(\lambda_i b) - I_0(\lambda_i a) K_0(\lambda_i b)} \tag{19}$$

$$R_i^*(r) = \frac{K_0(\lambda_i r)\, I_0(\lambda_i b) - I_0(\lambda_i r) K_0(\lambda_i b)}{K_0(\lambda_i a)\, I_0(\lambda_i b) - I_0(\lambda_i a) K_0(\lambda_i b)} \tag{20}$$

where K_0 is the modified Bessel function of second kind order zero; I_0 is the modified Bessel function of first kind order zero. C_i and D_i are the coefficients which will be determined by matching the potential and velocity at the common boundaries.

The eigenfunction in the vertical direction $Y(\lambda_i, z)$ is written as

$$Y(\lambda_i, z) = \begin{cases} 1 & \text{for } i = 0 \\ \sqrt{2}\cos\lambda_i z & \text{for } i \geq 1 \end{cases} \tag{21}$$

where $Y(\lambda_i, z)$ forms an orthogonal set in $[0, h - d]$.

The particular solution ϕ^{IIp}, subject to boundary conditions (13) and (14), is expressed as

$$\phi^{IIp}(r,z) = \frac{1}{2(h-d)}\left[z^2 - r^2/2\right] \tag{22}$$

The governing equation (12) and bottom condition (14) are also true in region III (replacing ϕ^{III} by ϕ^{II}).

In region III, ϕ^{III} also have to fulfil an appropriate radiation condition as $r \to \infty$, which has the form,

$$\lim_{r\to\infty} \sqrt{kr}\left(\frac{\partial \phi^{III}}{\partial r} - ik\phi^{III}\right) = 0 \tag{23}$$

where k is the wave number.

The solution in region III can be written as

$$\phi^{III}(r,z) = \sum_{j=0}^{\infty} B_j \Lambda^{III}(\chi_j, r)\, Z_p(\chi_j, z) \tag{24}$$

where B_j are unknown coefficients which will be determined by matching the boundary condition at the juncture boundary between regions II and III. χ_0 are the wave number related to ω through the dispersion relation,

$$\omega^2 = g\chi_0 \tanh(\chi_0 h_3) \tag{25}$$

where $h_3 = h_2 + h_1\rho_1/\rho_2$ and χ_j are positive roots of

$$\omega^2 = -g\chi_j \tan(\chi_j h_3)\ ,\ j \geq 1 \tag{26}$$

The eigenfunction in vertical direction $Z_p(\chi_j, z)$ can be written as

$$Z_p(\chi_j, z) = \begin{cases} \cosh(\chi_0 z) & \text{for } j = 0 \\ \cos(\chi_j z) & \text{for } j \geq 1 \end{cases} \tag{27}$$

where Z_p forms an orthogonal set in $[0, h_3]$.

Λ^{III} is the eigenfunction in the horizontal direction for region III, which is defined as

$$\Lambda^{III}(\chi_j, r) = \begin{cases} H_0(\chi_0 r)/H_0(\chi_0 b) & \text{for } j = 0 \\ K_0(\chi_j r)/K_0(\chi_j b) & \text{for } j \geq 1 \end{cases} \tag{28}$$

where H_0 is the Hankel function of the first kind order zero, chosen to satisfy the far-field radiation condition.

It is noteworthy that the solutions in all the three regions have to be matched at the adjoining boundaries. Therefore, the following conditions have to be applied on those boundaries.

On the adjoining boundary $r = a$,

$$\phi^{I(2)} = \phi^{II}\ ,\ 0 \leq z \leq h - d \tag{29}$$

$$\phi_r^{I(2)} = \phi_r^{II}\ ,\ 0 \leq z \leq h - d \tag{30}$$

$$\phi_r^{I(m)} = 0\ ,\ h - d \leq z \leq h \tag{31}$$

On the adjoining boundary $r = b$,

$$\phi^{III} = \phi^{II}\ ,\ 0 \leq z \leq h - d \tag{32}$$

$$\phi_r^{III} = \phi_r^{II}\ ,\ 0 \leq z \leq h - d \tag{33}$$

$$\phi_r^{III} = 0\ ,\ h - d \leq z \leq h_3 \tag{34}$$

Upon solving the boundary value problem by matching the solutions at the common boundaries, the five truncated groups of coefficients C_i, D_i, A_j^1, A_j^2, B_j can be obtained. The non-dimensional heave added mass and damping coefficients of the floating body are computed using the velocity potential on the wetted body surface

$$\mu_{33} + \mathrm{i}\lambda_{33} = \frac{1}{b^3}\int_0^{2\pi} \mathrm{d}\theta \int_a^b r\mathrm{d}r\ \phi^{II}(r, -d) \tag{35}$$

where μ_{33} and λ_{33} represent the heave added mass and damping coefficients, normalized by ρ_2, ω, b. In addition, both free surface and interfacial wave elevations inside and outside the pond can also be obtained.

3 Results and Discussions

An eigenfunction matching method is employed to solve the boundary value problem and ensure the mass and pressure continuity at the juncture boundaries between the three discrete fluid subdomains. The details of the numerical procedure can be referred to in [9, 10]. The proposed semi-analytical model has been validated through computing for a limiting case where $h_1/h_2 = 0.1$ and $\rho_1/\rho_2 = 0.2$, which is expected to be approaching to a single-layer moonpool problem. The obtained results are compared with the solutions for the corresponding single-layer case. The comparisons of added mass and damping are illustrated in Fig. 2. As shown, the present predictions for heave added mass and damping agree well with the results by Mavrakos [3]. In Fig. 2, Helmholtz (pumping mode) resonant frequency can be easily identified, where added mass changes the sign and damping coefficient goes to zero.

In order to examine the dependence of hydrodynamic behavior on density stratification and moonpool configuration, extensive parametric studies have been performed. Figs. 3 and 4 illustrates the effect of varying density ratio on the heave added mass and damping. As observed, in the high-frequency region, i.e. $Ka > 0.8$, the added mass for a higher density ratio is larger than that with a lower density ratio, which is expected. We also find that the density ratio can significantly affect Helmholtz resonance frequency. As seen in those figures, as density ratio increases, the Helmholtz resonance frequency decreases. In the low-frequency region, i.e. $Ka < 0.1$, both the added mass and damping coefficients increase with decreasing density ratio. It is also observed, as wave frequency decreases to zero, the damping coefficient is approaching to a constant value, while the added mass shows a singular behavior. This may be explained by the low-frequency asymptotics discussed in [6]. Furthermore, higher-order resonances can also be identified in Fig. 3, which can be associated with sloshing-like motion inside pond. As the density ratio increases, the higher-order resonance frequency and the bandwidth of the resonance decreases.

The modulus of the free-surface wave amplitudes (scaled by forcing amplitude) at $r = 0$, are presented in Fig. 5 for a typical moonpool configuration. As illustrated, two types of resonances can be recognized. One is associated with Helmholtz resonance and the other is related with a higher-order resonance. In order to understand the details of the resonance induced by the interfacial waves, a case with $\gamma = 0.7$ is chosen for further investigation. The internal wave amplitudes are plotted for a range of wave frequencies around the higher-order resonance frequency $Ka \approx 0.6783$. As illustrated in Fig. 6, as Ka approaches to 0.6783, the wave amplitude on the interface has been significantly amplified and a node, almost independent of the frequency, occurs at $r = 0.62$.

More results will be presented at the workshop including convergence tests, space-averaged wave amplitude inside moonpool, and far-field radiated waves.

References

[1] Chau, F. P. & Yeung, R. W. 2012 Inertia, damping, and wave excitation of heaving coaxial cylinders. In *Proc. of OMAE, Rio de Janeiro, Brazil*.

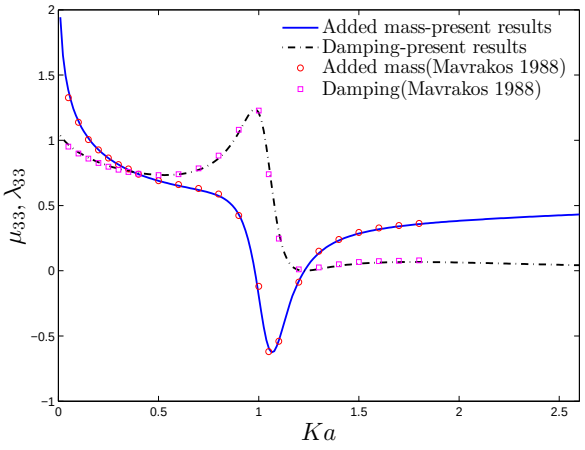

Figure 2: Heave added mass μ_{33} and damping coefficients λ_{33} versus non-dimensional wave frequency; depth ratio $h_1/h_2 = 1/10$, density ratio $\rho_1/\rho_2 = 0.2$, $b/a = 1.8$, draft $d/a = 1/3$

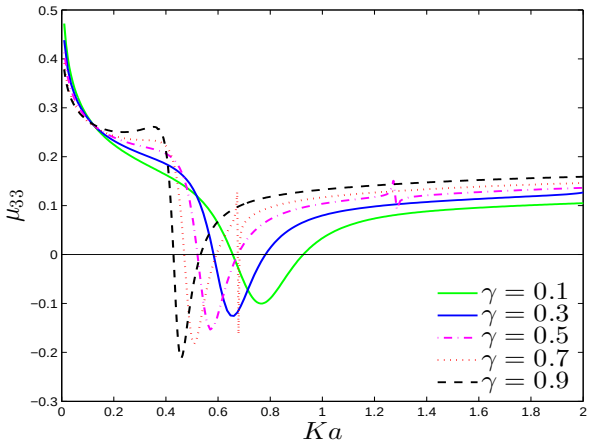

Figure 3: Dependence of heave added mass on density ratio; depth ratio $h_1/h_2 = 1.0$, $b/a = 1.2$, draft $d/h_1 = 1.5$, a/h_1=1.0

[2] Faltinsen, O. M., Rognebakke, O. F. & Timokha, A. N. 2007 Two-dimensional resonant piston-like sloshing in a moonpool. *J. of Fluid Mech.* **575**, 359–397.

[3] Mavrakos, S. A. 1988 Hydrodynamic coefficients for a thick-walled bottomless cylindrical body floating in water of finite depth. *Ocean Eng.* **15** (3), 84–97.

[4] Miloh, T. 1983 Wave loads on a floating solar pond. In *Proc. Int. Workshop on Ship and Platform Motions, Dept of Nav. Arch. and Offshore Eng., UC Berkeley, California*.

[5] Molin, B. 2001 On the piston sloshing modes in moonpools. *J. of Fluid Mech.* **430**, 27–50.

[6] Yeung, R. W. 1981 Added mass and damping of a vertical cylinder in finite-depth waters. *Applied Ocean Res.* **3**, 119–133.

[7] Yeung, R. W. & Nguyen, T. 1999 Waves generated by amoving source in a two-layer ocean of finite depth. *J. of Eng. Math.* **35**, 85–107.

[8] Yeung, R. W. & Seah, R. K. M. 2007 On helmholtz and higher-order resonance of twin floating bodies. *J. of Eng. Math.* **58** (1-4), 251–265.

[9] Zhang, X. & Bandyk, P. 2013 On two-dimensional moonpool resonance for twin bodies in a two-layer fluid. *Applied Ocean Res.* **40**, 1–13.

[10] Zhang, X. & Bandyk, P. 2014 Two-dimensional moonpool resonances for interface and surface-piercing twin bodies in a two-layer fluid. *Applied Ocean Res.* **47**, 204–218.

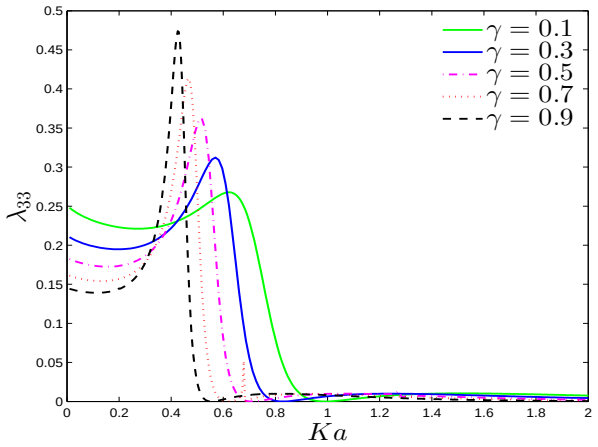

Figure 4: Dependence of heave damping on density ratio; depth ratio $h_1/h_2 = 1.0$, $b/a = 1.2$, draft $d/h_1 = 1.5$, a/h_1=1.0

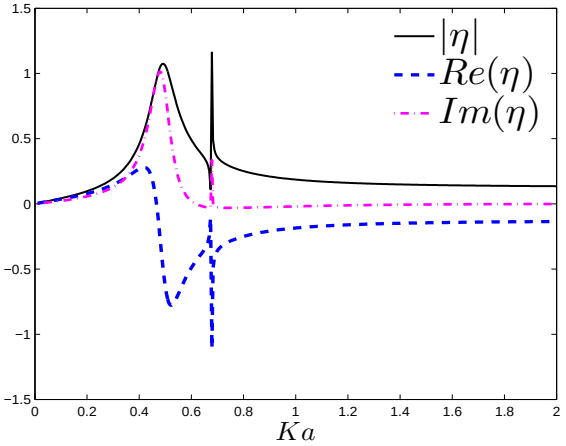

Figure 5: Free surface wave amplitude at $r = 0$ versus Ka; depth ratio $h_1/h_2 = 1.0$, $b/a = 1.2$, draft $d/h_1 = 1.5$, a/h_1=1.0, $\gamma = 0.7$

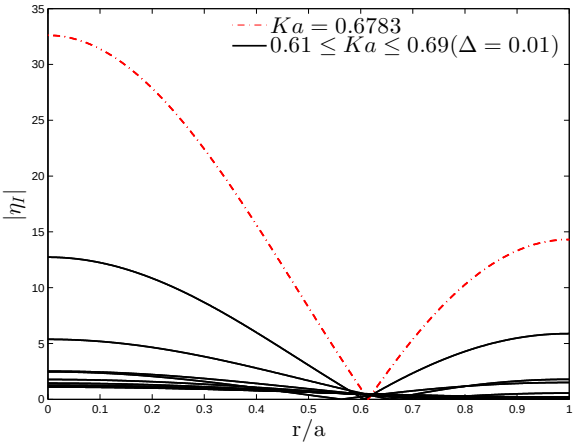

Figure 6: Wave amplitude $|\eta_I|$ on interfacial surface for different forcing frequencies; depth ratio $h_1/h_2 = 1.0$, $b/a = 1.2$, draft $d/h_1 = 1.5$, a/h_1=1.0, $\gamma = 0.7$